

# Structure of basic winged-bean lectin and a comparison with its saccharide-bound form

N. Manoj, V. R. Srinivas and K. Suguna\*

Molecular Biophysics Unit, Indian Institute of Science, Bangalore-560 012, India

Correspondence e-mail:  
suguna@mbu.iisc.ernet.in

The crystal structure of the saccharide-free form of the basic form of winged-bean agglutinin (WBAI) has been solved by the molecular-replacement method and refined at 2.3 Å resolution. The final *R* factor is 19.7% for all data in the resolution range 8.0–2.3 Å. The asymmetric unit contains two half-dimers, each located on a crystallographic twofold axis. The structure of the saccharide-free form is compared with that of the complex of WBAI with methyl- $\alpha$ -D-galactoside. The complex is composed of two dimers in the asymmetric unit. The intersubunit interactions in the dimer are nearly identical in the two structures. The binding site of the saccharide-free structure contains three ordered water molecules at positions similar to those of the hydroxyl groups of the carbohydrate which are hydrogen bonded to the protein. Superposition of the saccharide-binding sites of the two structures shows that the major changes involve expulsion of these ordered water molecules and a shift of about 0.6 Å of the main-chain atoms of the variable loop.

Received 17 November 1998

Accepted 8 January 1999

**PDB Reference:** saccharide-free basic form of winged-bean lectin, 1wbf.

## 1. Introduction

Lectins, a class of multivalent proteins, specifically recognize and bind carbohydrates. This ability has led to their diverse biological properties and widespread applications in biochemistry, cell biology and medicine (Sharon & Lis, 1989; Rini, 1995). Lectins isolated from plant sources, in particular those of the family *leguminosae*, have been studied best. The members of this family share a highly conserved three-dimensional structure but differ significantly in their sugar specificity and oligomerization. Legume lectins are classified based on the type of carbohydrates they bind to, *viz.* mannose/glucose, galactose/*N*-acetyl-galactosamine, fucose, *N*-acetyl-glucosamine/chitobiose or complex sugars. Crystal structures are available for galactose-binding lectins such as *Erythrina corallodendron* lectin (EcorL; Shaanan *et al.*, 1991), peanut lectin (Banerjee *et al.*, 1994, 1996), soybean agglutinin (Dessen *et al.*, 1995), WBAI (Prabu *et al.*, 1998), glucose/mannose-binding lectins such as concanavalin A (con A; Hardman & Ainsworth, 1972; Deacon *et al.*, 1997), pea lectin (Einspahr *et al.*, 1986), *Lathyrus ochrus* isolectin I (LOLI; Bourne, Abergel *et al.*, 1990) and lentil lectin (Loris *et al.*, 1993), and complex binding lectins such as lectin IV from *Griffonia simplicifolia* (GS4; Delbaere *et al.*, 1993) and phytohaemagglutinin L (Hamelryck *et al.*, 1996). However, subtle but significant differences in carbohydrate specificities exist within each class. Crystal structures of a number of legume lectin–saccharide complexes and some saccharide-free forms have been determined (Loris *et al.*, 1998). Coordinates of con A, LOLI, pea lectin, GS4, lentil lectin and EcorL are available in both the

saccharide-bound and unbound forms from the Protein Data Bank (Bernstein *et al.*, 1977).

The crystal structure of WBAI in complex with methyl- $\alpha$ -D-galactoside was solved at 2.5 Å by Prabu *et al.* (1998) and the details of the saccharide-binding site were reported. The binding site is made up of four loops and, as in other legume lectins, three of them (78–87, 95–117 and 124–137) are substantially conserved, while the fourth loop (211–222), of variable sequence and length, determines the specificity (Sharma & Suroliya, 1997). There is a network of six hydrogen bonds connecting atoms O3, O4 and O6 of the galactoside to residues Asn128, Gly105, Asp87, Asp212 and His84. A water molecule bridges the O2 atom to Gly105 and Asp128 through hydrogen bonds.

We now report the structure of the saccharide-free form of WBAI, a 56 kDa glycosylated dimeric lectin and provide a detailed comparison with the structure of the complex.

## 2. Materials and methods

### 2.1. Crystallization and data collection

WBAI was isolated and crystallized as described previously (Khan *et al.*, 1986; Sankaranarayanan *et al.*, 1993). X-ray diffraction data were collected at room temperature on a 300 mm MAR Research image-plate detector mounted on a Rigaku RU-200 X-ray generator operated at 40 kV and 50 mA. Diffraction data to 2.3 Å resolution were collected as a series of discrete frames, each comprising of 0.5° oscillation and an exposure time of 720 s using a crystal-to-detector distance of 155 mm. The data were indexed, integrated and scaled using the *MARXDS* suite of programs (Kabsch, 1988). The crystal belongs to the monoclinic space group *C2* with two monomers per asymmetric unit, giving a  $V_m$  of 3.3 Å<sup>3</sup> Da<sup>-1</sup> (Matthews, 1968). The unit-cell parameters and other details of data collection are shown in Table 1. This is a new crystal

**Table 1**

Crystallographic data and details of data collection.

Crystal dimensions (mm)	0.5 × 0.3 × 0.1
Space group	<i>C2</i>
Unit-cell parameters	
<i>a</i> (Å)	99.16
<i>b</i> (Å)	75.16
<i>c</i> (Å)	95.77
$\beta$ (°)	106.9
Radiation used	Cu <i>K</i> $\alpha$
Resolution (Å)	2.3
Number of observations	38947
Number of unique reflections	26671
Data completeness (%)	
29.0–2.3 Å	88.6
2.4–2.3 Å	80.6
$\langle I/(\sigma I) \rangle$	
29.0–2.3 Å	12.5
2.4–2.3 Å	2.8
$R_{\text{merge}}$ (%) <sup>†</sup>	7.3
$R_{\text{merge}}$ in the last shell (%)	35.9

<sup>†</sup>  $R_{\text{merge}} = \sum_{hkl} |I_i - \langle I \rangle| / \sum \langle I \rangle$ , where  $I_i$  is the  $i$ th intensity measurement and  $\langle I \rangle$  is the mean intensity for the reflection.

form, different to the orthorhombic form with two dimers in the asymmetric unit reported earlier (Sankaranarayanan *et al.*, 1993).

### 2.2. Structure solution

*AMoRe* (Navaza, 1994) was used to solve the structure of WBAI. A monomer of the dimeric WBAI complexed with a monosaccharide (Prabu *et al.*, 1998) refined to an  $R$  value of 18.0% at 2.5 Å resolution (PDB code 1WBL) was used as the search model. The metal ions, the N-linked carbohydrates and all water molecules were removed from the initial model. The rotation search was carried out using intensity data in the resolution range 15–5 Å. The first two peaks in the rotation-function map, with correlation coefficient values of 0.213 and 0.171, correspond to the two monomers in the asymmetric unit. Using these two solutions, single-body translation searches were carried out in the same resolution range and unique solutions were obtained. In order to find the relative positions of these two solutions, a two-body translation search was carried out. The positions of the molecules of the asymmetric unit were then refined with the rigid-body option of *AMoRe*. As a result, an  $R$  factor of 0.336 and a correlation coefficient of 0.683 were obtained.

The initial model, oriented and positioned according to the molecular-replacement solution, was examined on a graphics system with the program *O* (Jones *et al.*, 1991). As shown in Fig. 1, the two subunits *A* and *B* in the asymmetric unit belong to two different dimers of WBAI. Even though the subunits are related by a non-crystallographic twofold axis, this does not give rise to the formation of the functional dimer between them. The

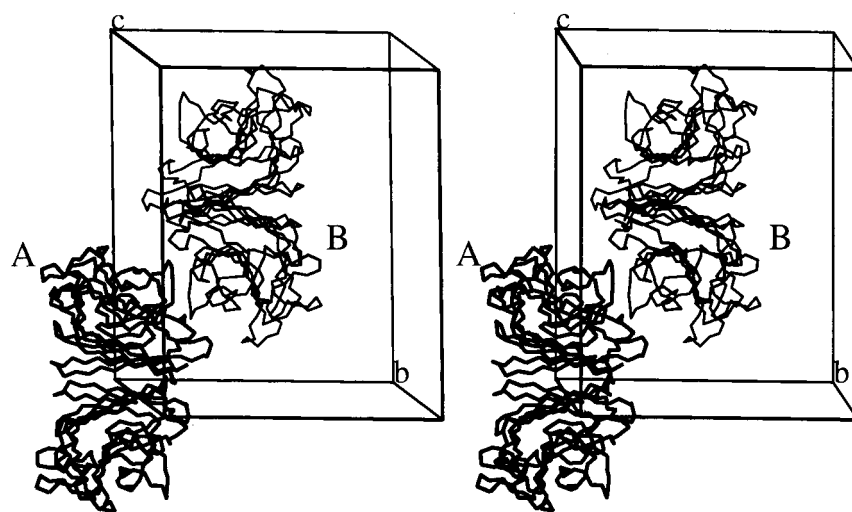


**Figure 1**

Stereo diagram of the two molecules *A* (thick) and *B* (thin) in the unit cell as viewed down the non-crystallographic twofold axis. The dimers of WBAI are generated by the crystallographic twofold axes along and parallel to *b*.

dimers of WBAI are located on two crystallographically independent dyads.

### 2.3. Refinement

The protein model obtained by molecular replacement was refined by the *X-PLOR* program, version 3.1 (Brünger, 1992a), initially using intensity data to 3.0 Å. Progress of the refinement was monitored using the free *R* factor (Brünger, 1992b) with 8% of the reflections randomly removed from the data set. After 15 cycles of rigid-body refinement the *R* factor was 31.2%. Regular positional refinement of the model employing non-crystallographic symmetry (NCS) restraints was carried out for a few cycles. Metal ions, one Ca<sup>2+</sup> and one Mn<sup>2+</sup> per monomer, were then added on inspection of  $2F_o - F_c$  and  $F_o - F_c$  electron-density maps. The data set was then expanded to include data in the resolution range 8–2.3 Å, and the NCS restraints were progressively relaxed and then removed in further cycles of positional refinement. Manual checking and rebuilding of the model was performed using the program *O* (Jones *et al.*, 1991) at several stages of the refinement. Several cycles of positional refinement yielded an *R* factor of 26.3% and an  $R_{\text{free}}$  of 31.5%. At this stage, individual restrained *B* factors of the protein atoms were refined.  $2F_o - F_c$  and  $F_o - F_c$  Fourier maps were calculated using the refined coordinates, and water molecules and N-linked carbohydrates were added. Only the first sugar ring of the heptasaccharide [Man $\alpha$ 6(Man $\alpha$ 3)Xyl $\beta$ 2Man $\beta$ 4GlcNAc $\beta$ 4(L-Fuca $\alpha$ 3)GlcNAc $\beta$ ] could be located in the electron-density maps at residues Asn44 and Asn219, to which it is covalently linked. A 1/8th omit map (Vijayan, 1980; Bhat & Cohen, 1984) was computed to remove possible ambiguities arising from model bias. Successive positional and individual restrained *B*-factor refinements reduced the *R* factor to 19.7% ( $R_{\text{free}} = 25.6\%$ ) with intensity data in the 8.0–2.3 Å resolution range (Table 2). The final structure was evaluated by construction of a Ramachandran plot (Ramachandran & Sasisekharan, 1968) using the *PROCHECK* package (Laskowski *et al.*, 1993) and a Luzzati plot (Luzzati, 1952).

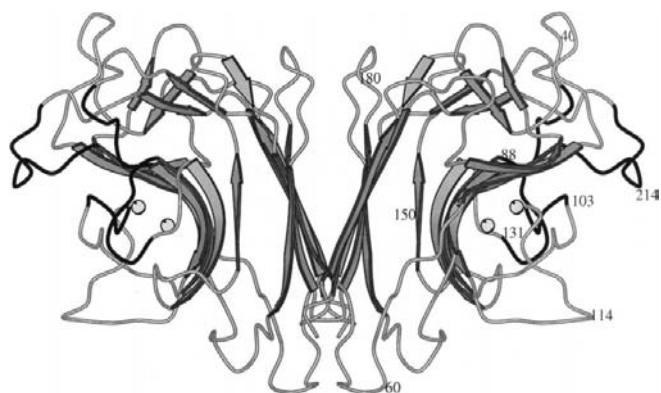


**Figure 2**  
The dimer of WBAI. The calcium and manganese ions are shown as spheres. The carbohydrate-binding loops are coloured black. This figure, Fig. 3 and Fig. 5 were generated using the program *MOLSCRIPT* (Kraulis, 1991).

**Table 2**  
Final refinement statistics.

Protein atoms in the model	3622
Solvent atoms	283
N-linked sugar atoms	56
Other ions	2Mn, 2Ca
<i>R</i> factor (for all data) (%)	19.7
$R_{\text{free}}$ (%)	25.6
Resolution (Å)	8.0–2.3
$B_{\text{ave}}$ (Å <sup>2</sup> )	29.6
R.m.s. deviations	
Bond distances (Å)	0.01
Bond angles (°)	1.72
Dihedrals (°)	28.12
Impropers (°)	1.49
Ramachandran plot statistics	
Residues in most favoured regions out of a total of 796 non-glycine and non-proline residues (%)	83.6

## 3. Results and discussion

### 3.1. Structure description

The tertiary and the quaternary structures of WBAI in the saccharide-free and the ligand-bound forms are essentially identical. Each subunit has the same characteristic legume-lectin fold resulting from three  $\beta$ -sheets: a six-stranded flat-back  $\beta$ -sheet, a seven-stranded curved-front  $\beta$ -sheet and a small five-stranded  $\beta$ -sheet connecting the first two (Fig. 2). The root-mean-square (r.m.s) deviations of the main-chain atoms between the two forms are 0.45 and 0.43 Å for subunit *A* and subunit *B*, respectively. The geometry of the calcium and manganese-binding sites, including the coordinating water molecules, is also very similar in the two structures. Furthermore, the *cis* peptide linkage between residues Ala86 and Asp87, which coordinates the Ca<sup>2+</sup> ion, is also conserved.

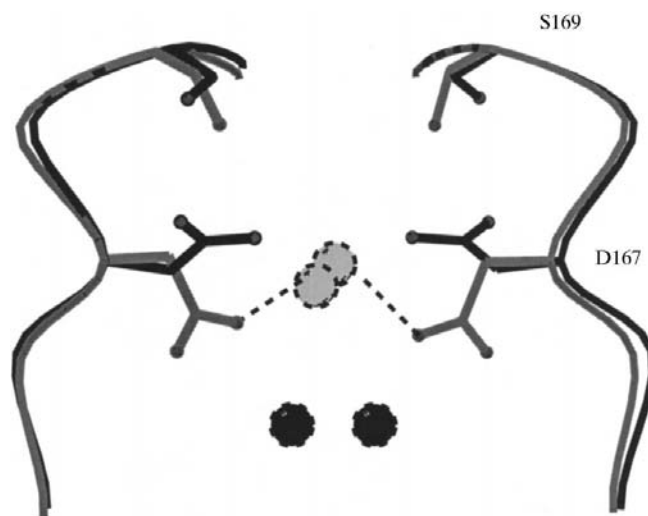


**Figure 3**  
The dimer interface showing small differences between the ligand-bound (grey) and free (black) forms of WBAI.

**Table 3**Average atomic  $B$  factors ( $\text{\AA}^2$ ) of main-chain atoms.

All main-chain atoms

Saccharide-free form	
Subunit <i>A</i>	29.0
Subunit <i>B</i>	28.0
Complex	16.4

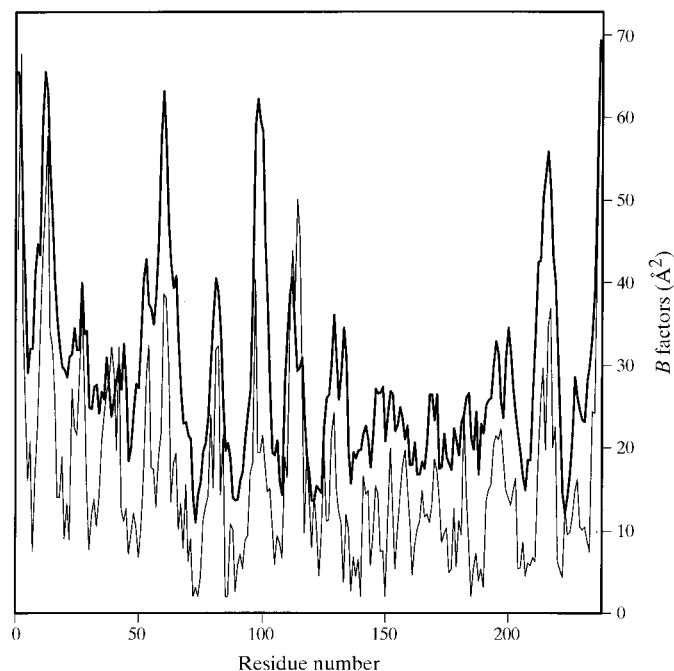
Saccharide-binding loops

Saccharide free form	
Subunit <i>A</i>	27.2
Subunit <i>B</i>	26.2
Complex	14.0

The two subunits of each WBAI dimer are related by crystallographic dyads in the saccharide-free form. In contrast, the dimers in the complex are formed by local non-crystallographic dyads. The dimeric association in the two structures is, however, almost identical. The inter-subunit interactions within each dimer comprise ten hydrogen bonds, four bridging water molecules, one of which is exactly on the twofold axis, and seven hydrophobic interaction pairs. In the structure of the complex, eight of these ten hydrogen bonds, six of the seven hydrophobic interaction pairs and four of the five water bridges are conserved. However, minor differences have been observed in the conformations of the side chains of Asp167 and Ser169 at the dimer interface, which results in the loss of a water bridge present in both the dimers in the complex (Fig. 3).

The average atomic  $B$  factors of the main-chain atoms in each subunit of the saccharide-free form and that of the liganded form are shown in Table 3. The average  $B$  factor of

the saccharide-free protein is considerably higher than that of the complex. This could be a consequence of the less compact packing of this form in the crystal structure, as reflected by a higher solvent content (61%) compared with that (44%) of the complex. A similar comparison in the case of con A showed that in the ligand-bound structure, the average temperature factors of the subunits were increased and a slight loosening of the subunits within the tetramer (Naismith *et al.*, 1994) has been observed. However, a comparison of the average  $B$  factors of the saccharide-binding loops with that for a whole subunit (Table 3) shows that the saccharide binding does not significantly affect the ordering of the binding loops relative to the bulk of the subunit. A similar observation has been made in the case of con A. The  $B$  factors averaged over the main-chain atoms are shown in Fig. 4 for subunit *A*. It can be seen from this figure that the  $B$  factors of loop 110–117 are significantly lower than those of the same loop in the complex. A detailed comparison of the two structures shows a considerable movement of the main-chain atoms (r.m.s. deviation of 1.0  $\text{\AA}$ ) and significant differences in the side-chain conformations of this loop, as shown in Fig. 5. It has been observed that these differences are a consequence of the involvement of this loop in intermolecular contacts in the saccharide-free form. About two-thirds of a total of 66 crystal contacts ( $<4.0$   $\text{\AA}$ ) are made by this loop. Also shown in Fig. 5 is the conformational change which occurs in the side chain of another residue, Tyr106, which plays a role in strengthening the binding interaction between WBAI and C2-substituted carbohydrates (Swaminathan *et al.*, 1997; Prabu *et al.*, 1998). This residue could also contribute to the binding of *N*-dansyl derivatives (Khan *et al.*, 1986) to WBAI, as in the case of EcorL (Arango *et al.*, 1993; Adar *et al.*, 1998).

**Figure 4**

Atomic  $B$  factors averaged over the main-chain atoms for molecule *A* (thick line) and for the galactoside complex (thin line).

### 3.2. Saccharide-binding site

Comparison of the carbohydrate-binding site of the galactoside complex with both of the crystallographically independent molecules of the saccharide-free structure shows that on ligand binding the 211–218 loop shifts towards the carbohydrate, resulting in r.m.s. displacements of 0.6  $\text{\AA}$  in the positions of the backbone atoms (Fig. 6). Similar displacements were observed in the pea lectin (Rini *et al.*, 1993) and LOLI (Bourne, Rouge *et al.*, 1990; Bourne, Roussel *et al.*, 1990) complexes. The shift towards the carbohydrate in the loop position enables hydrogen-bond formation between the backbone NH group of Asp212 and the carbohydrate O4 atom. No difference in either the main-chain or in the side-chain conformations has been observed between the two structures for the other three loops of the carbohydrate-binding region.

In addition, alignment of the structures shows that three water molecules are displaced on carbohydrate binding. Two water molecules, OW1 and OW2, which are common to both subunits, are very close to the positions of the O3 and O4 atoms of the galactoside complex and in fact make the same hydrogen-bond interactions with the protein. A third water molecule OW3, corresponding to the position O6 of the

saccharide and making the same hydrogen bond to the protein, is observed only in subunit *B* (Fig. 7). Although the thermodynamic significance of displacing these water molecules is unclear, the conservation of geometry with respect to

the O3, O4 and O6 groups certainly reflects the preformed character of this region. Water molecules occupying the positions of hydroxyl groups of the carbohydrates in order to preserve the hydrogen-bonding interactions in the sugar-binding region have also been

observed in the structures of other legume lectins (Rini *et al.*, 1993; Bourne, Rouge *et al.*, 1990; Bourne, Roussel *et al.*, 1990; Delbaere *et al.*, 1993; Elgavish & Shaanan, 1998; Ravishankar *et al.*, 1998).

Superposition of the carbohydrate-binding sites in both the structures shows that OW1, OW2 and OW3 are 0.73, 0.69 and 0.35 Å away from O3, O4 and O6, respectively, in subunit *B*. This type of shift in the water positions and the movement of the variable loop in WBAI supports the observation made by Elgavish & Shaanan (1998) that these two parameters are correlated. They also pointed out, based on the structures available, that these shifts occur only in the glucose/mannose-binding lectins, with the exception of con A, and that similar changes have not taken place in galactose-binding lectins (EcorL and GS4). WBAI is a galactose-binding lectin and yet shows shifts in the variable loop and the water positions, suggesting that either WBAI is another exception to the general observation or, as mentioned by Elgavish & Shaanan (1998), more structures are needed before arriving at any general conclusions. One possible reason for the movement of the variable loop in WBAI could be the length of this loop. Examination of the variable loops in different legume lectins shows that this loop is the longest in WBAI (Sharma & Surolia, 1997). Prabu *et al.* (1998) showed that the length of the loop plays a key role in conferring specificity to WBAI.

There are other differences in the water structures of the saccharide-binding sites. One is the presence of a water molecule in both subunits of the saccharide-free form, hydrogen bonded to Asp212 O and Gln217 O and thus stabilizing the variable loop (Fig. 8). In subunit *B*, this water molecule bridges the water molecule OW3 and the main-chain atoms. Also,

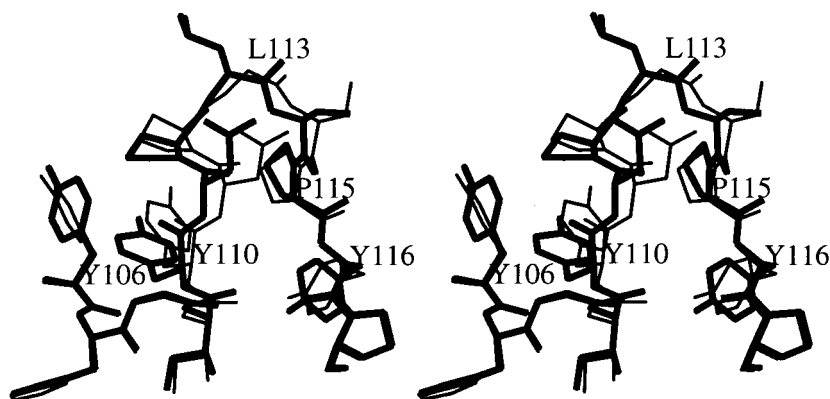


**Figure 5**  
Superposition of the loops containing residues 106–117 in the two structures of WBAI (saccharide-free form as thick lines and the complex as thin lines) to show the main-chain movement and the differences in side-chain conformations.

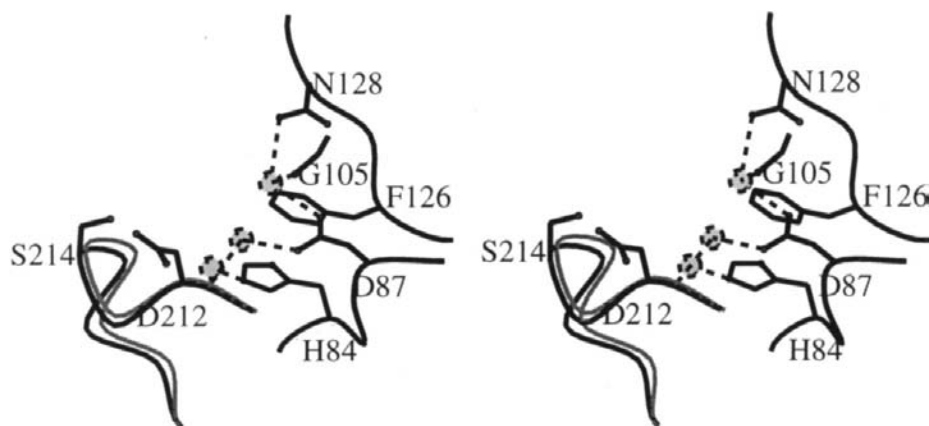


**Figure 6**  
Stereoview of the carbohydrate-binding region of the saccharide-free form of WBAI. The variable loop of the ligand-bound form (grey) is also shown.

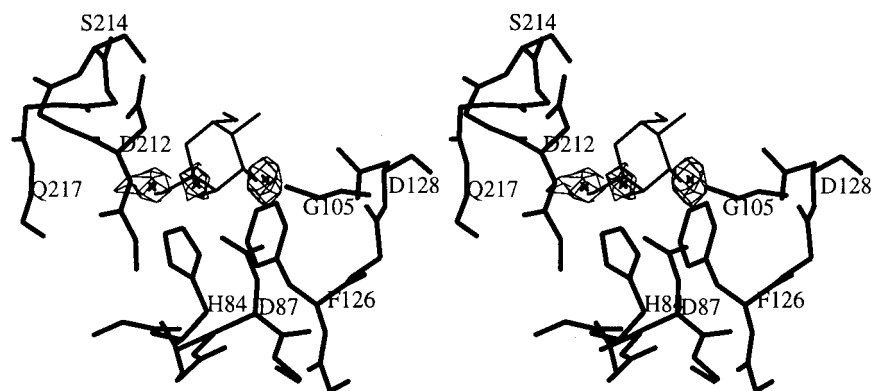


**Figure 7**  
Stereoview showing the density of water molecules located in the carbohydrate-binding region of the saccharide-free form of WBAI. These water molecules occupy the positions of O3, O4 and O6 of methyl- $\alpha$ -D-galactose (thin lines) bound to WBAI in the complex.

the water bridge connecting O2 of the saccharide to Gly105 N and Asn128 ND2 in the structure of the complex (Prabu *et al.*, 1998) is absent in the saccharide-free form.

### 3.3. Hydration

The final refined model has 283 water molecules. A distance criterion of 3.6 Å was applied for a water molecule to be considered as interacting with an O or N atom to form a hydrogen bond. When this condition is applied, 45 water molecules do not interact with any other molecule, while 45 were found to make contact only with other water molecules. The remaining 193 water molecules interact with protein atoms.

A comparison of the hydration of the two crystallographically independent subunits was carried out. As in the case of our earlier studies on protein hydration (Kodandapani *et al.*, 1990; Madhusudan & Vijayan, 1991; Radha Kishan *et al.*, 1995; Banerjee *et al.*, 1996), a water molecule of one subunit was considered to be invariant to one of the other subunit if they interacted with at least one common protein atom and if the distance between the two was less than 1.8 Å when the two

subunits along with their hydration shells were superposed on each other. Accordingly, a total of 57 water molecules were found to be invariant between the subunits. In particular, it is instructive to examine the extent to which the hydration shell of the subunits of the saccharide-free form of WBAI reflects that of the complex.

A comparison of the hydration of the subunits of the saccharide-free and the complex structures showed 25 invariant water molecules. These water molecules include the six which were found to exist in the structures of all legume lectins and their complexes by Loris *et al.* (1994). Four of them are involved in metal coordination and one of these also interacts with protein atoms which hydrogen bond to the carbohydrate ligand. Of the remaining two, one stabilizes the 141–145 loop while the other bridges the loops 52–67 and 192–203. Four bridging water molecules are present at the subunit interface, with one of them located on the twofold axis of the dimer. The loops bearing the N-glycosylation sites are stabilized by one water molecule. The loops 77–88 and 125–135, which are involved in carbohydrate recognition, are bridged by a network of three water molecules (Fig. 9). One water molecule interconnects the strands of the third sheet, and five water molecules are associated with the top loops. Two water molecules are exclusively associated with the back sheet and two water molecules are associated with the bottom loops connecting the back and the front sheets.

As many as 12 invariant water molecules, including the four which coordinate to the metal ions, are found in the region made up of the loops at the top and the adjoining sheets. For example, three water molecules which connect two carbohydrate-binding loops are shown in Fig. 9. It is perhaps significant that a majority of the invariant water molecules occur in this region, providing additional stability to these loops and ensuring the correct structural relations among them necessary for carbohydrate binding.

We thank Professors M. Vijayan and A. Surolia for their interest and suggestions. The intensity data were collected at the National Data Collection Facility at the Institute, supported by the Departments of Science and Technology (DST), and Biotechnology, Government of India. The computations were performed at the Supercomputer Education and Research Centre of the Institute. NM acknowledges financial support from the University Grants Commission. This work was funded by the DST.

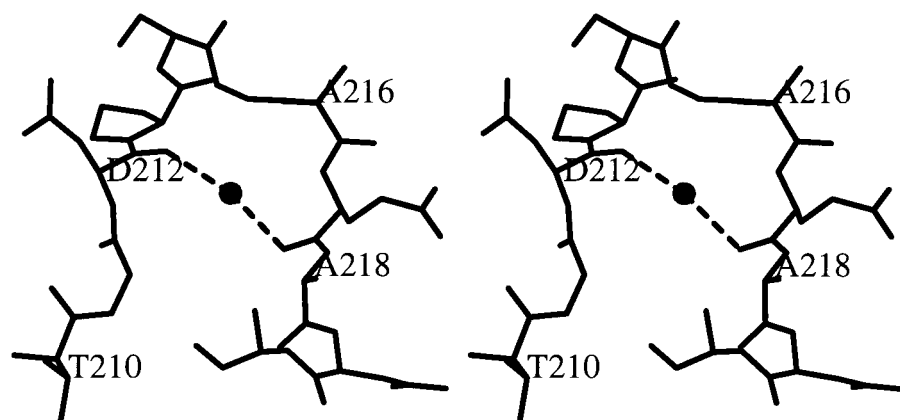


**Figure 8**  
Stereoview of the variable loop stabilized by a water molecule found only in the saccharide-free form of WBAI.

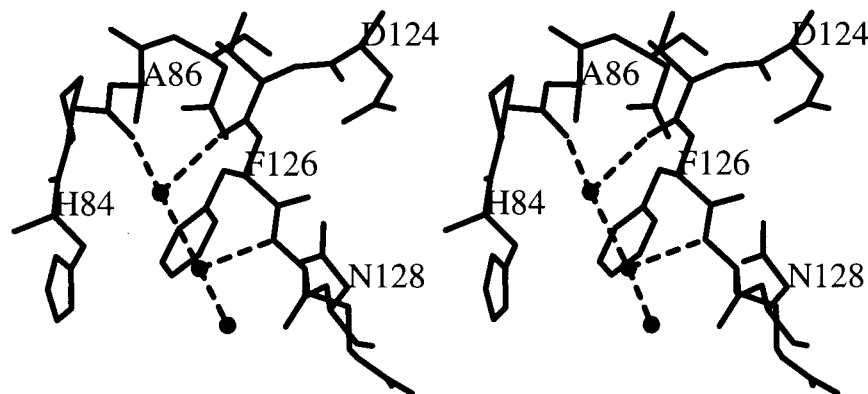


**Figure 9**  
Stereo diagram showing three water molecules stabilizing two of the carbohydrate-binding loops.

References

- Adar, R., Moreno, E., Streicher, H., Karlsson, K.-A., Ångström, J. & Sharon, N. (1998). *Protein Sci.* **7**, 52–63.
- Arango, R., Rodriguez-Arango, E., Adar, R., Belenky, D., Loontjens, F., Rozenblatt, S. & Sharon, N. (1993). *FEBS Lett.* **330**, 133–136.
- Banerjee, R., Das, K., Ravishankar, R., Suguna, K., Surolia, A. & Vijayan, M. (1996). *J. Mol. Biol.* **259**, 281–296.
- Banerjee, R., Mande, S. C., Ganesh, V., Das, K., Dhanaraj, V., Mahanta, S. K., Suguna, K., Surolia, A. & Vijayan, M. (1994). *Proc. Natl Acad. Sci. USA*, **91**, 227–231.
- Bernstein, F. C., Koetzle, T. F., Williams, G. J. B., Meyer, E. F. Jr, Brice, M. D., Rodgers, J. R., Kennard, O., Shimanouchi, T. & Tasumi, M. (1977). *J. Mol. Biol.* **112**, 535–542.
- Bhat, T. N. & Cohen, G. H. (1984). *J. Appl. Cryst.* **17**, 244–248.
- Bourne, Y., Abergel, C., Cambillau, C., Frey, M., Rouge, P. & Fontecilla-Camps, J. C. (1990). *J. Mol. Biol.* **214**, 571–584.
- Bourne, Y., Rouge, P. & Cambillau, C. (1990). *J. Biol. Chem.* **265**, 18161–18165.
- Bourne, Y., Roussel, A., Frey, M., Rouge, P., Fontecilla-Camps, J. C. & Cambillau, C. (1990). *Proteins Struct. Funct. Genet.* **8**, 365–376.
- Brünger, A. T. (1992a). *X-PLOR Version 3.1. A System for Crystallography and NMR*. Yale University, New Haven, Connecticut, USA.
- Brünger, A. T. (1992b). *Nature (London)*, **355**, 472–475.
- Deacon, A., Gleichmann, T., Kalb (Gilboa), A. J., Price, H., Raftery, J., Bradbrook, G., Yariv, J. & Helliwell, J. R. (1997). *J. Chem. Soc. Faraday Trans.* **93**, 4305–4312.
- Delbaere, L. T. J., Vandonselaar, M., Prasad, L., Quail, J. W., Wilson, K. S. & Dauter, Z. (1993). *J. Mol. Biol.* **230**, 950–965.
- Dessen, A., Gupta, D., Sabesan, S., Brewer, C. F. & Sacchettini, J. C. (1995). *Biochemistry*, **34**, 4933–4942.
- Einspahr, H., Parks, E. H., Suguna, K., Subramanian, E. & Suddath, F. L. (1986). *J. Biol. Chem.* **261**, 16518–16527.
- Elgavish, S. & Shaanan, B. (1998). *J. Mol. Biol.* **277**, 917–932.
- Hardman, K. D. & Ainsworth, C. F. (1972). *Biochemistry*, **11**, 4910–4919.
- Hamelryck, T. W., Dao-Thi, M.-H., Poortmans, F., Chrispeels, M. J., Wyns, L. & Loris, R. (1996). *J. Biol. Chem.* **271**, 20479–20485.
- Jones, T. A., Zou, J. Y., Cowan, S. W. & Kjeldgaard, M. (1991). *Acta Cryst.* **A47**, 110–119.
- Kabsch, W. (1988). *J. Appl. Cryst.* **21**, 916–924.
- Khan, M. I., Sastry, M. V. K. & Surolia, A. (1986). *J. Biol. Chem.* **261**, 3013–3019.
- Kodandapani, R., Suresh, C. G. & Vijayan, M. (1990). *J. Biol. Chem.* **265**, 16126–16131.
- Kraulis, P. J. (1991). *J. Appl. Cryst.* **24**, 946–950.
- Laskowski, R. A., MacArthur, M. W., Moss, D. S. & Thornton, J. M. (1993). *J. Appl. Cryst.* **26**, 283–291.
- Loris, R., Hamelryck, T., Bouckaert, J. & Wyns, L. (1998). *Biochim. Biophys. Acta*, **1383**, 9–36.
- Loris, R., Stas, P. P. G. & Wyns, L. (1994). *J. Biol. Chem.* **269**, 26722–26733.
- Loris, R., Steyaert, J., Maes, D., Lisgarten, J., Pickersgill, R. & Wyns, L. (1993). *Biochemistry*, **32**, 8772–8781.
- Luzzati, V. (1952). *Acta Cryst.* **5**, 802–810.
- Madhusudan & Vijayan, M. (1991). *Curr. Sci.* **60**, 165–170.
- Matthews, B. W. (1968). *J. Mol. Biol.* **33**, 491–497.
- Naismith, J. H., Emmerich, C., Habash, J., Harrop, S. J., Helliwell, J. R., Hunter, W. N., Raftery, J., Gilboa, A. J. K. & Yariv, J. (1994). *Acta Cryst.* **D50**, 847–858.
- Navaza, J. (1994). *Acta Cryst.* **A50**, 157–163.
- Prabu, M. M., Sankaranarayanan, R., Puri, K. D., Sharma, V., Surolia, A., Vijayan, M. & Suguna, K. (1998). *J. Mol. Biol.* **276**, 787–796.
- Radha Kishan, K. V., Chandra, N. R., Sudarsanakumar, C., Suguna, K. & Vijayan, M. (1995). *Acta Cryst.* **D51**, 703–710.
- Ramachandran, G. N. & Sasisekharan, V. (1968). *Adv. Protein Chem.* **23**, 283–438.
- Ravishankar, R., Suguna, K., Surolia, A. & Vijayan, M. (1998). Personal communication.
- Rini, J. M. (1995). *Annu. Rev. Biophys. Biomol. Struct.* **24**, 551–557.
- Rini, J. M., Hardman, K. D., Einspahr, H., Suddath, F. L. & Carver, J. P. (1993). *J. Biol. Chem.* **268**, 10126–10132.
- Sankaranarayanan, R., Puri, K. D., Ganesh, V., Banerjee, R., Surolia, A. & Vijayan, M. (1993). *J. Mol. Biol.* **229**, 558–560.
- Shaanan, B., Lis, H. & Sharon, N. (1991). *Science*, **254**, 862–866.
- Sharma, V. & Surolia, A. (1997). *J. Mol. Biol.* **267**, 433–445.
- Sharon, N. & Lis, H. (1989). *Science*, **246**, 227–246.
- Swaminathan, C. P., Gupta, D., Sharma, V. & Surolia, A. (1997). *Biochemistry*, **36**, 13428–13434.
- Vijayan, M. (1980). *Computing in Crystallography*, pp. 19.01–19.26. Bangalore: Indian Academy of Sciences.